Photomechanical investigations on the stress-strain relationship in dentine macrostructure

A. Kishen
National University of Singapore
Department of Restorative Dentistry
Faculty of Dentistry
Singapore 119704, Republic of Singapore

A. Asundi
Nanyang Technological University
School of Mechanical and Production Engineering
Singapore 639798, Republic of Singapore

Abstract. In this study photomechanical experiments were carried out to examine the relationship between macroscopic mechanical stress and strain gradients within the root dentine structure. Three-dimensional digital photoelasticity was used to study the stress distribution patterns in tooth models, while digital moiré interferometry was used to study the strain gradients within the natural teeth. The stress analysis showed a distinct bending stress distribution, along faciolingual plane in the coronal and cervical regions of the tooth. There was a reduction in bending towards the apical third of the tooth model. The strain analysis displayed strain gradients in the axial (along the long axis of the tooth) and lateral (perpendicular to the long axis of the tooth) directions in dentine. There was a conspicuous reduction in strains from the cervical to the apical third of the root dentine. The root dentine displayed uniform distribution of normal strains. Although there was a steep increase in stresses from the inner core region to the outer surface of an isotropic tooth model, there were more uniform strain gradients in the natural dentine structure. It is apparent from these observations that complex organization of material properties facilitated distinct strain gradients in dentine structure during mechanical functions. [DOI: 10.1117/1.1924688]

Keywords: digital photoelasticity; digital moiré interferometry; dentine; stress; strain.

Paper 04162 received Aug. 17, 2004; revised manuscript received Dec. 14, 2004; accepted for publication Dec. 15, 2004; published online May 27, 2005.

1 Introduction

Different studies in the past have emphasized complex anisotropy in the material properties of dentine.[1] Yet very few attempts were made to understand the nature of anisotropy and to establish a structure to material property relationship in dentine. Such studies will aid in approximating the requirements on artificial biomaterials when used to replace lost tooth structure. It is established that isotropic ''artificial'' restorative material when used to restore anisotropic ''natural'' dentine, would consistently result in lack of functional harmony between the restoration and the remaining tooth structure.[2] This will lead to micromovement of the restoration and loss of marginal integrity at the tooth-restoration interface, which are established signs of failures in dental restorations.

It is understood that a biological structure balances its functional requirements with its achieved anatomical optimizations.[3] This aspect has been well established in the case of bone tissues. Wolff first observed this process in bone and termed it as the process of functional adaptation. Wolff's theory of functional adaptation states that for every change in the form and function or function alone, there will be a definite change in the internal and the external architecture of osseous tissue in accordance with mathematical laws.[4] Studies have shown that mechanical stresses and strains produce preeminent stimulus that regulates material properties and subsequently maintain functional requirements in bone tissue.[5,6]

Dentine is a mineralized tissue rather similar to bone, in which collagen rich organic matrix is reinforced by calcium phosphate mineral particles. However, unlike bone, dentine does not remodel once it is fully mineralized. The microstructure of this composite structure has been recently studied, and these studies have shown that the mechanical properties of dentine are dominated by intertubular dentin.[7,8] Previous studies have also highlighted a strong correlation between the increase in mechanical properties, thickness of mineral crystal, and concentration of minerals.[7,9] However, any specific patterns of functional adaptation from a macrostructural perspective has not been investigated in detail.

The major limitation associated with the understanding of mechanical characteristics in dentine is related to the presence of dissimilar phases namely minerals (carbonated apatite), collagen and water (bound and unbound), and all of them demonstrating very different mechanical characteristics.[10–12] In addition, studies have highlighted variations in the microstructure of collagen and mineral crystals in different regions of the dentine structure.[8,13] Previous microindentation experi-

Address all correspondence to Anil Kishen. Tel: (65) 6874 4624; Fax: (65) 6774 5701; E-mail: rsdak@nus.edu.sg

1083-3668/2005/$22.00 © 2005 SPIE

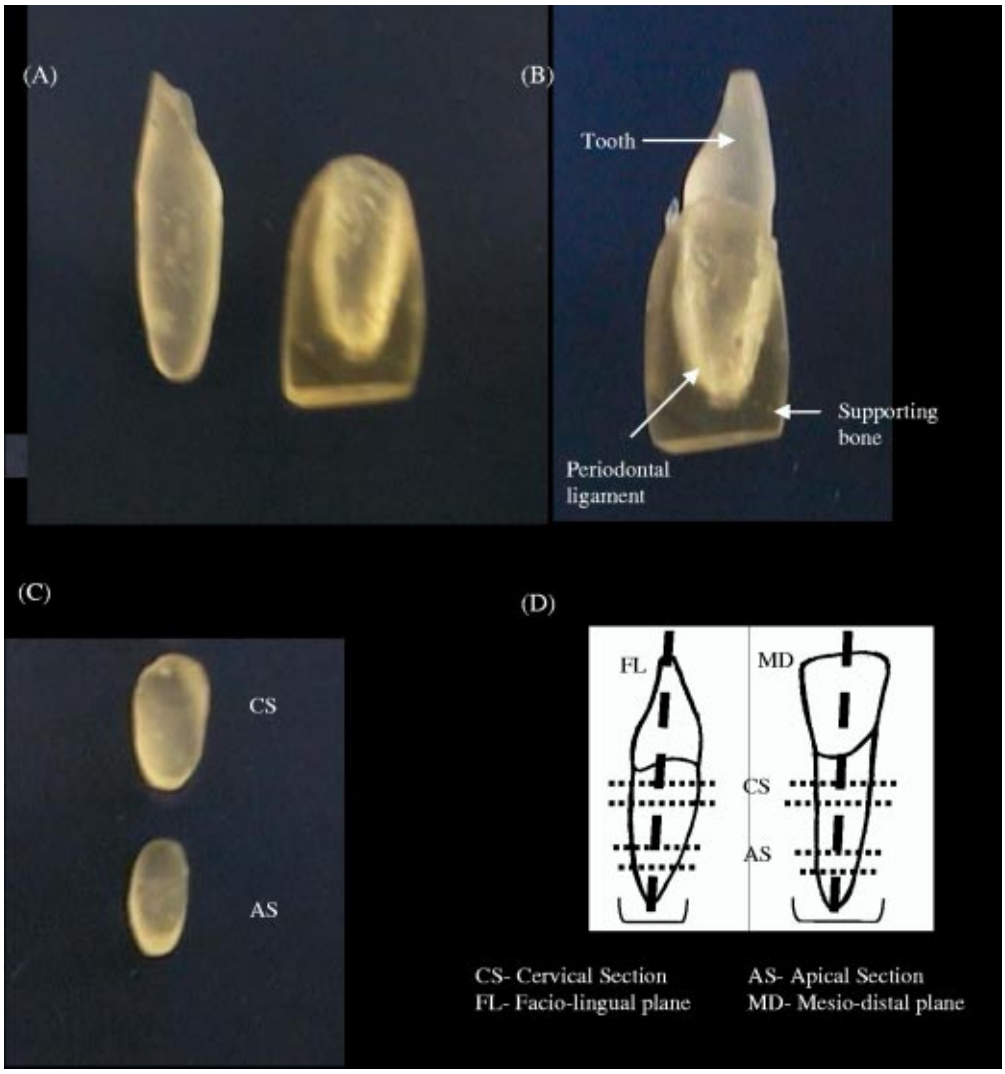

Fig. 1 Three-dimensional photoelastic models of (a) the tooth and supporting bone separated, (b) the tooth-supporting bone models interfaced by silicon rubber to simulate periodontal ligament, (c) the cross sections at the cervical and apical regions of the tooth, and (d) the schematic diagram showing different tooth sections and anatomical planes.

ments and fluoroscopic x-ray microscopic imaging analysis have displayed a methodical gradient in elastic modulus, along the faciolingual plane in dentine.[14] This study aims to investigate the evidence of relationship between stress-strain distribution and material organization in human dentine from a macrostructural perspective. It is achieved by utilizing a three-dimensional digital photoelasticity that provides complete-field stress distribution pattern in tooth models, and a digital moiré interferometry that provides complete-field strain gradients within dentine. The stress distribution pattern obtained from isotropic tooth models is compared with the strain gradients observed in anisotropic natural tooth structure to understand the influence of material organization on the stress-strain distribution within dentine structure.

2 Experiments

2.1 *Three-Dimensional Digital Photoelastic Analysis: Stress Distribution Pattern*

Three-dimensional digital photoelasticity was conducted in four stages. In the first stage, models were prepared using a photoelastic liquid resin. In the second stage, the models were subjected to postcure cycle. In the third stage, the models were subjected to a stress-freezing procedure. In the fourth stage, the stress frozen models were sectioned along different planes of interest and analyzed in a circular polariscope using a four-step phase shift technique.

The models were prepared using a liquid resin system supplied as two liquids consisting of a resin and a hardener (PLM-1, Measurements Group, Inc.). During model preparation a human mandible with anterior dentition obtained from an adult cadaver was sectioned distal to the lateral incisors on the left and right side. The central incisors were then carefully extracted from the socket and replicating molds of the mandible and the central incisor were prepared using silicone rubber base impression material (PROVIL, Bayer Dental). Subsequently, 12 parts by weight of hardener was taken with 100 parts of resin and mixed well until the temperature (exothermic reaction) rose to 52 °C. At that temperature, the liquid epoxy was poured into the previously prepared mold.

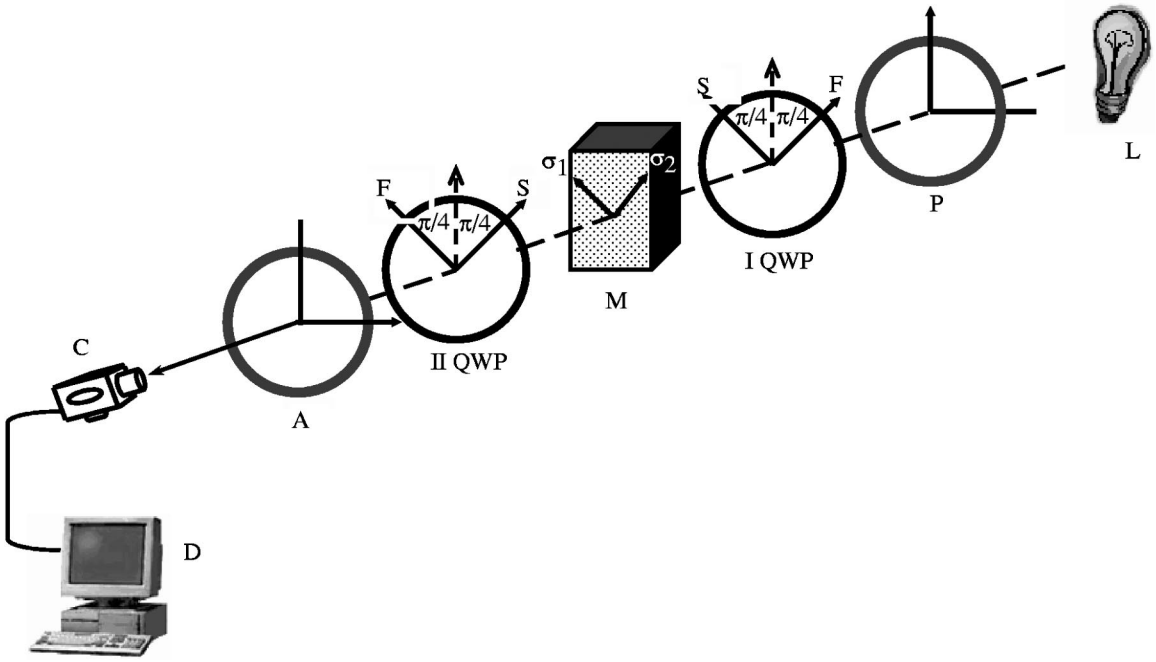

Fig. 2 Schematic diagram of a digital photoelastic experimental arrangement.

The initial polymerization of resin was completed in 24 h after pouring into the mold. The models were next subjected to a postcure cycle. The postcure cycle consisted of heating the models along with the silicone rubber mold in an oven for up to 80 °C at a rate of 5 °C/h. The plastic was then maintained at this temperature for 2 h and then cooled to room temperature at the rate of 5 °C/h. Following this cycle, the photoelastic models were ready for stress freezing.[15] The entire manipulation of the photoelastic material (PLM-1) was carried out in accordance to the manufacturer's instruction. These steps ensured proper curing of photoelastic plastic and aid in achieving the prescribed properties of PLM-1.[16]

Models of mandibular central incisor and supporting bone models were individually prepared for this study (Fig. 1), and this facilitated simulation of periodontal ligament at the tooth-bone interface. Models were prepared based on the relative modulus of elasticity of different dento-osseous structures. Photoelastic liquid plastic (PLM-1) with elastic modulus of 2.9 GPa was used to prepare the tooth and the supporting bone models. A layer of chemically cured silicon rubber, 0.35 mm thick, and an elastic modulus of 0.2 MPa, was used to simulate the periodontal ligament. A polyester reinforced composite sheet 0.15 mm thick simulated the root cementum. This sheet had an elastic modulus that was similar to that of photoelastic models but with higher resilience. The earlier thickness for silicon rubber and polyester composite sheet was chosen to replicate the original anatomical dimensions of periodontal ligament and cementum. Since the objective of this study was to evaluate the stress distribution pattern in structural dentine, the model materials were chosen keeping in mind the relative elastic modulus difference between the anatomic structures.[17]

Three teeth and supporting bone models, and a calibration disk were prepared from a single batch of photoelastic liquid plastic. The models and the calibration disk were next subjected to a stress-freezing procedure. The stress-freezing procedure was an important step in three-dimensional photoelasticity. During stress-freezing, the models were subjected to loads at a specific elevated temperature. The load induced stress patterns were then frozen within the model during the cooling phase. In this study the model was gradually heated to 125 °C, and was loaded. A loading jig was designed and fabricated to hold the anatomically scaled models within an oven. An experimental load of 10 N was applied along the long axis of the tooth model at 125 °C. This load was chosen due to the lower stiffness of the model material at higher temperature. Further, a pilot study showed that this load was sufficient to produce optimum number of fringes for the sectional model analysis. The temperature of 125 °C was maintained for 2 h to facilitate uniform softening of the entire model material. This stage was followed by a cooling phase. The entire stress-freezing procedure was carried out at a rate of 5 °C/h. The value of the stress-optic coefficient at the stress freezing temperature was determined from the calibration disc (14 kPa/fringe m).

After the stress-freezing cycle, the tooth model was separated from the bone model and was cross sectioned along different regions of interest at the cervical third and apical

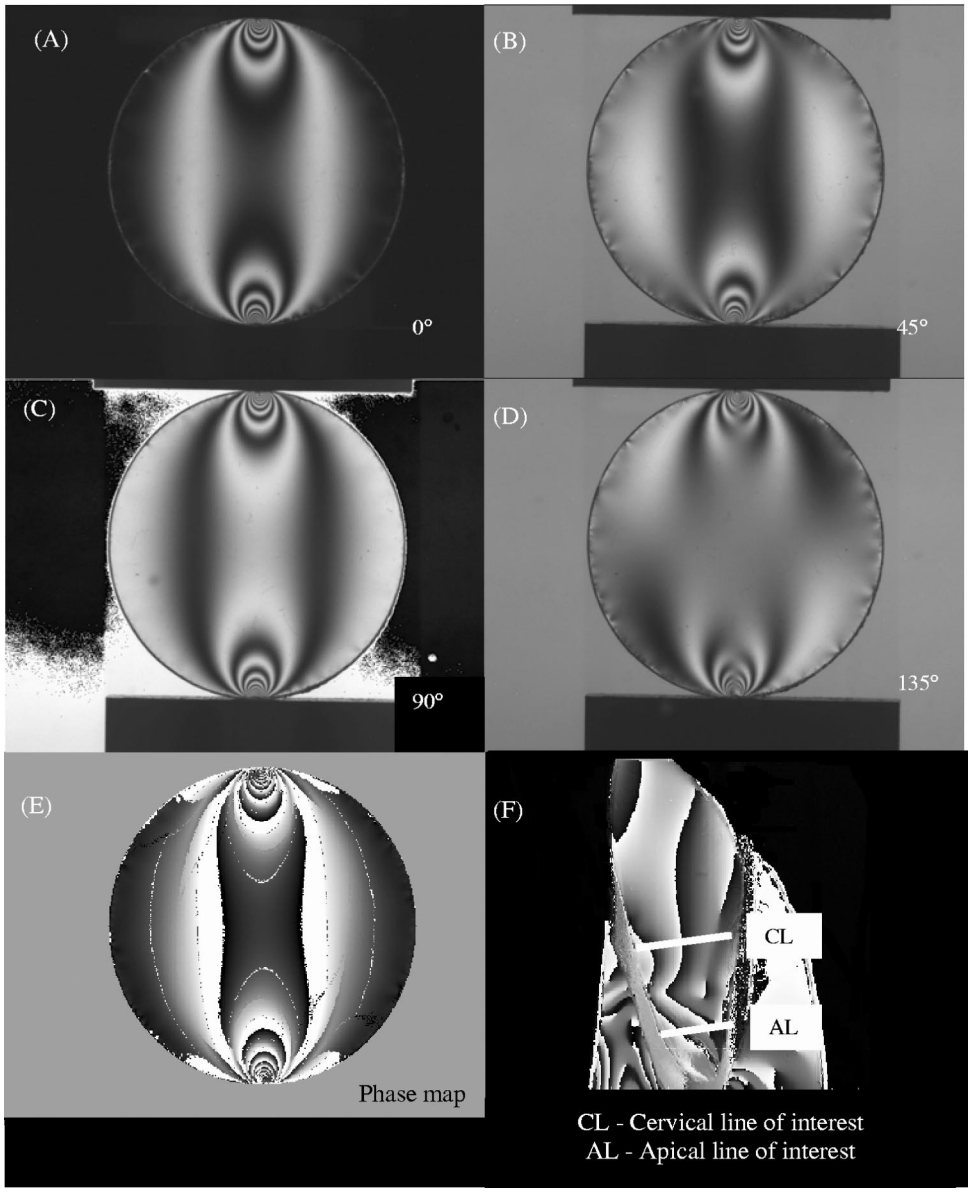

Fig. 3 Shows the phase shifted images of a calibration disc obtained by rotating the analyzer's axis of polarization with respect to the polarizer's axis of polarization for (a) 0°, (b) 45°, (c) 90°, and (d) 135°, in a circular polariscope (e) the phase wrapped image obtained from the four phase shifted images and (f) the phase wrapped map of the tooth and the supporting bone (sagittal section).

third of the tooth [Fig. 1(d)]. Sectioning of the models was carried out immediately after stress freezing using a diamond-impregnated wheel, mounted on a milling machine with distilled water as a coolant. The sectioned, stress-frozen models were then placed between the first and the second quarter-wave plate of a circular polariscope, and the fringe patterns were recorded using a charge coupled device (CCD) camera (Fig. 2). In digital photoelasticity, rotating the analyser at 0°, 45°, 90°, and 135° with respect to the polarizer induced the four phase steps [Figs. 3(a), 3(b), 3(c), and 3(d)]. These four phase-shifted images were evaluated using a phase unwrapping algorithm, in order to obtain the wrapped phase map [Fig. 3(e)]. Further details regarding the digital photoelastic fringe analyzis is presented elsewhere.[17]

The stress distribution obtained from the wrapped phase map look similar to a conventional fringe pattern, but displayed phase information rather than intensity information of the fringes. Phase unwrapping was carried out along selected lines in the wrapped image to make the fringe modulation continuous and to obtain details on the absolute nature and magnitude of stress distribution. The phase unwrapping method is based on modulation ordering and relies on the intensity modulation in pixels.[17] In this study the stress patterns along the faciolingual plane (sagittal plane) were evaluated before sectioning the models, whereas the stress patterns along the cross sections were evaluated after sectioning the models.

2.2 *Digital Moiré Interferometric Analysis: Strain Gradients*

Specimens for the moiré interferometric analysis were prepared from three permanent noncarious mandibular incisor

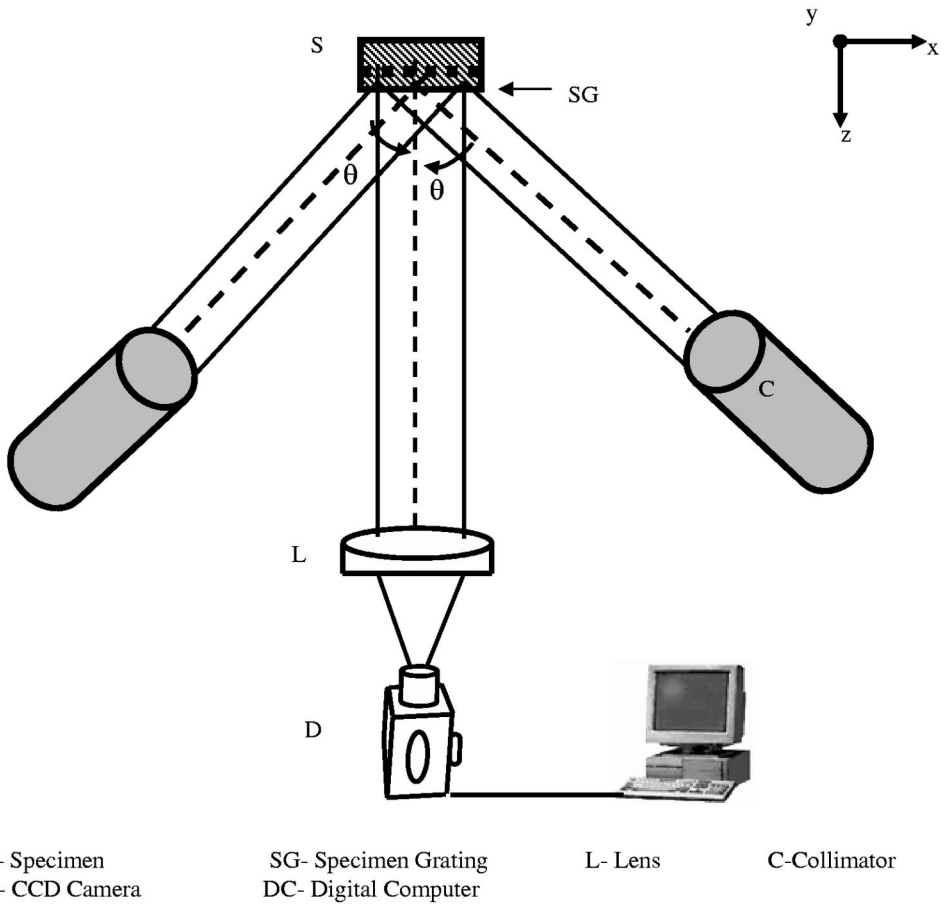

Fig. 4 Schematic diagram of the digital moiré interferometry experimental arrangement.

teeth, stored in phosphate buffered saline solution immediately following extraction. The specimens were transilluminated prior to testing to exclude possibilities of cracks and were tested within 3 weeks of extraction. The teeth specimens for the moiré investigation were prepared by grinding the mesial and distal surfaces on wet emery papers of grit size 180, 400, 800, and 1000 to obtain parallel-sided, sagittal sections with a uniform thickness of 2.5 mm.

Moiré methods utilize grating as a deformation-sensing element. To prepare the specimen grating, a high frequency grating from a mold was transferred onto the surface of the specimen using a thin layer of epoxy adhesive (PC-10, Measurements Group, Raleigh, NC). This specimen grating was interrogated using a virtual reference grating formed by the interference of two mutually coherent beams incident on the specimen plane at a fixed angle (Fig. 4). Moiré fringes result from the interference between the deformed specimen grating and the virtual reference grating. These fringes represent contour maps of in-plane displacement fields and were analyzed using image processing software. Further details on the specimen grating preparation are presented in Post et al.[18]

The experiment consisted of the following four stages.

A high frequency cross grating ($f=1200$ lines/mm) was replicated on one faciolingual surface (sagittal side) of the tooth section using epoxy adhesive at room temperature. The replication was done in such a way that the grating lines were parallel and perpendicular to the long axis of the tooth. The distance between the adjacent grating lines is referred to as the pitch of the grating, which in this case was 0.833 μm. The specimen with the replicated grating was mounted on a horizontal loading jig that permitted compressive loading of the tooth specimen. The loading jig is designed with a load cell, which was connected to a digital display that aided in monitoring the applied load. The loading jig was subsequently positioned in the moiré interferometer (Fig. 4).

The moiré interferometer was used to visualize the resulting load induced deformation fringes. The moiré interferometer consisted of two mutually coherent light beams from a diode laser ($\lambda=670$ nm) which were incident on the specimen grating at an oblique angle and generated a virtual reference grating of 2400 lines/mm [corresponding to a pitch (P) of 0.417 μm]. This virtual reference grating interacted with the deformed specimen grating to produce the moiré fringe patterns. A high resolution CCD camera (Electrim 1000HR, NJ) was used to digitize and record the fringe patterns obtained for further analysis.

Moiré fringes represent contours of displacement components in the direction perpendicular to the lines of the grating. Hence, during our experiments the surface displacements along the x axis, known as U field and that along the y axis, known as V field were obtained by rotating the specimen in the interferometer to enable the specimen grating lines perpendicular to the x and y axis to interact with the virtual reference grating individually (Fig. 5). During experiments

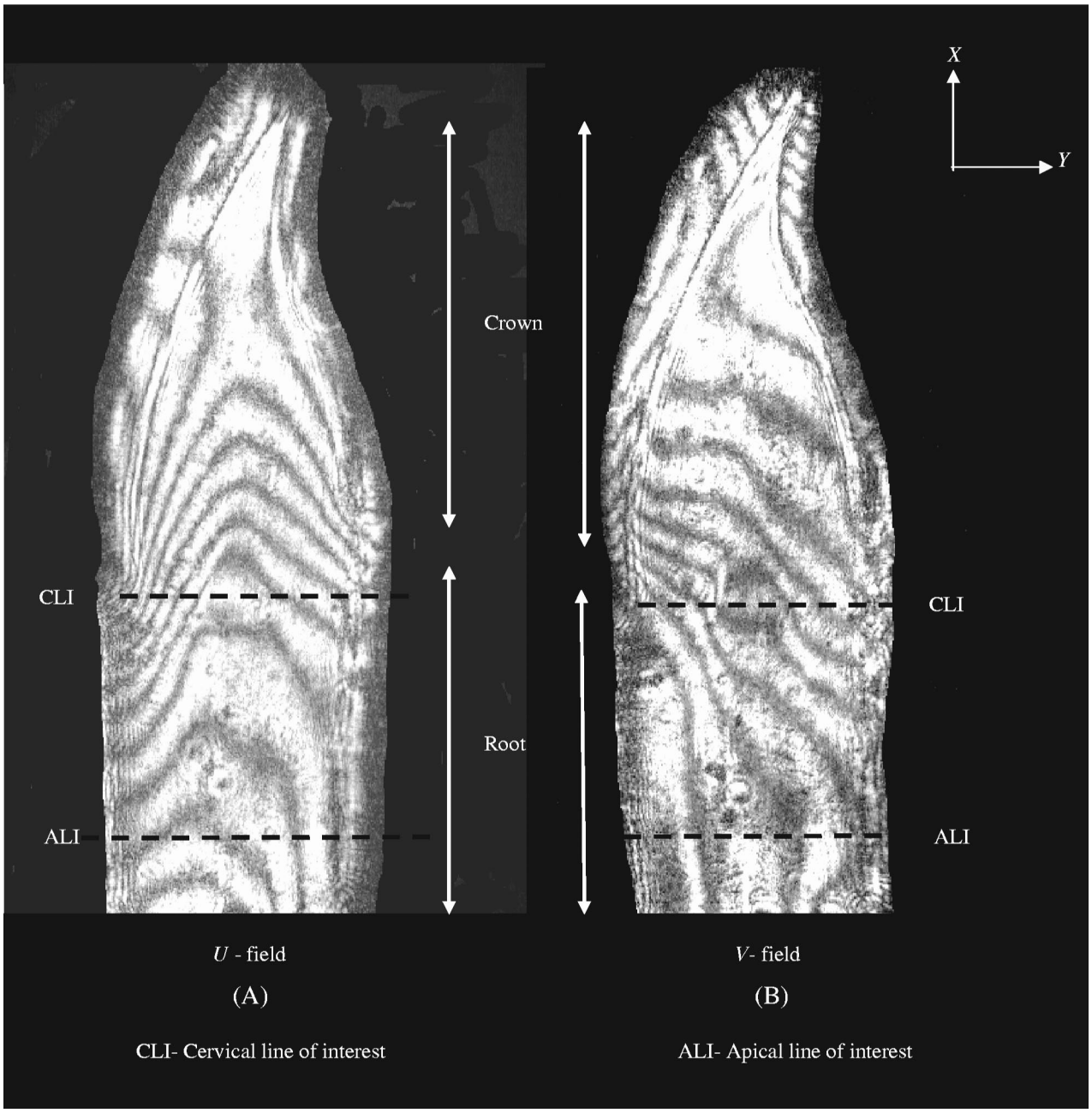

Fig. 5 Typical image showing (a) the *U* field (deformation in the axial direction) and (b) the *V* field (deformation in the lateral direction) moiré fringe patterns.

compressive loads of 10, 20, and 30 N were applied at the incisal edge, along the long axis of the tooth, and the moiré fringes were acquired.

Strain is a geometric quantity, which depends on the relative movements of two or three points in a body. Strains in experimental mechanics are technically classified as: normal and shear strains. A normal strain is defined as the change in length of a line segment between two points divided by the original length of the line segment. A shear strain is defined as the angular change between two line segments, which are originally perpendicular. The normal and the shear strain gradients for each load, along selected lines of interest in the cervical and apical dentine (Fig. 5) were determined as follows.

From the *U* field fringe pattern the normal strain (ε_x) in *x* direction (axial direction/along the long axis of the tooth) is given as:

$$\frac{\Delta U}{\Delta x} = \varepsilon_x = \frac{P}{\Delta x}, \tag{1}$$

where ΔU is the relative displacement component in the *x* direction between two points. If the two points are on adjacent fringes then $\Delta U = P$, which is the pitch of the reference grat-

ing. To obtain the normal strain in the x direction, divide P by Δx, the spacing between the two fringes in the x direction.

Similarly $\Delta U/\Delta y$ can be written as

$$\frac{\Delta U}{\Delta y}=\frac{P}{\Delta y}, \tag{2}$$

where Δy is the spacing between two adjacent fringes in the y direction.

From the V-field fringe pattern, the normal strain (ε_y) in the y direction can be deduced as

$$\frac{\Delta V}{\Delta y}=\varepsilon_{y'}=\frac{P}{\Delta y'}, \tag{3}$$

where ΔV is the y component of the in-plane displacement, $\Delta y'$ is the fringe spacing in the y direction (lateral direction/perpendicular to the long axis of the tooth). We can also determine $\Delta V/\Delta x'$ from

$$\frac{\Delta V}{\Delta x}=\frac{P}{\Delta x'}, \tag{4}$$

where $\Delta x'$ is the spacing between the adjacent fringes in the x direction.

The shear strain (γ_{xy}) is then given as

$$\gamma_{xy}=\frac{\Delta V}{\Delta x}+\frac{\Delta U}{\Delta y}=\frac{P}{\Delta x'}+\frac{P}{\Delta y}. \tag{5}$$

3 Results

3.1 *Three-Dimensional Digital Photoelastic Analysis: Stress Distribution Pattern*

It was found that the applied compressive loads resulted in a distinct bending stress at the coronal and cervical region of the tooth model. The bending stress resulted in low stress at the inner region, which increased towards the facial and lingual surfaces [Fig. 6(a)]. Bending stress is produced in structures subjected to eccentric load (loads acting away from the line of symmetry). Bending results in a transition of stress (or strain) from tensile to compression, passing through a zero at neutral axis. A conspicuous reduction in bending was observed at the apical region of the tooth [Fig. 6(b)].

Figures 7(a) and 7(b) are phase wrapped images showing the stress distribution at the cross sections from the cervical and middle third of the tooth model. The cervical cross section displayed conspicuous distribution of bending stresses along the faciolingual plane [Figs. 7(c) and 7(d)]. These stresses increased from the inner region towards the outer surfaces. The facial surface displayed higher stress compared to the lingual side. The cross section at the apical dentine showed less signs of bending and revealed more uniform distribution of stresses. The magnitude of stresses at the apical region was lower than that in the cervical region.

3.2 *Digital Moiré Interferometric Analysis: Strain Gradients*

The U field (axial strain) and V field (lateral strain) moiré analyses showed that the compressive loads resulted in a distinct distribution of normal and shear strains along the axial and lateral directions in the dentine [Figs. 5(a) and 5(b)]. The outer aspect of the coronal and cervical dentine exhibited prominent axial strains during compression. The U field analysis showed that the initial loads on the tooth produced conspicuous distribution of axial strains at the cervical dentine. These strains at the cervical dentine were both normal and shear in nature [Figs. 8(a) and 8(b)]. The facial aspect of the cervical dentine displayed shear strains adjacent to the cemento-enamel junction [Fig. 8(b)]. The root dentine, which was apical to the cervical region, did not display noticeable strains for loads less than 20 N. However, at 30 N load there was a uniform distribution of normal strains in root dentine [Fig. 8(c)]. In root dentine, there was no shear strain in this direction. The normal axial strains in the apical dentine were lower than the normal axial strains in the cervical dentine [Fig. 8(d)].

The V field analysis showed strain distribution in the lateral direction (perpendicular to the long axis) in the dentine. The cervical dentine displayed predominant distribution of lateral strains. The lateral strains in the cervical dentine were both normal and shear in nature [Figs. 9(a) and 9(b)]. The root dentine demonstrated uniform distribution of the normal strains in this direction [Fig. 9(c)]. There were no shear strains in the lateral direction in root dentine. The normal lateral strains in the apical dentine were lower than the normal lateral strains in the cervical dentine [Fig. 9(d)].

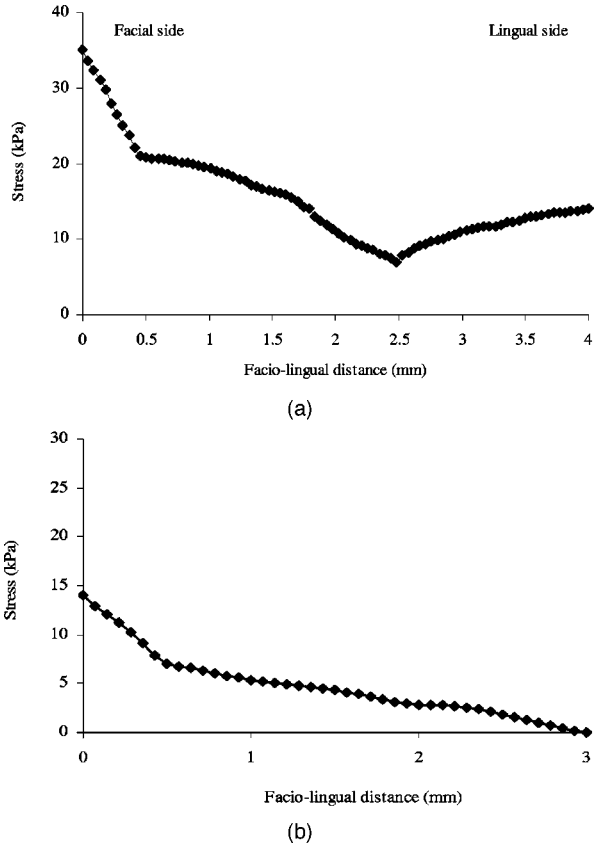

Fig. 6 Typical graphs showing the stress distribution pattern in the sagittal plane at the (a) cervical and (b) apical dentine.

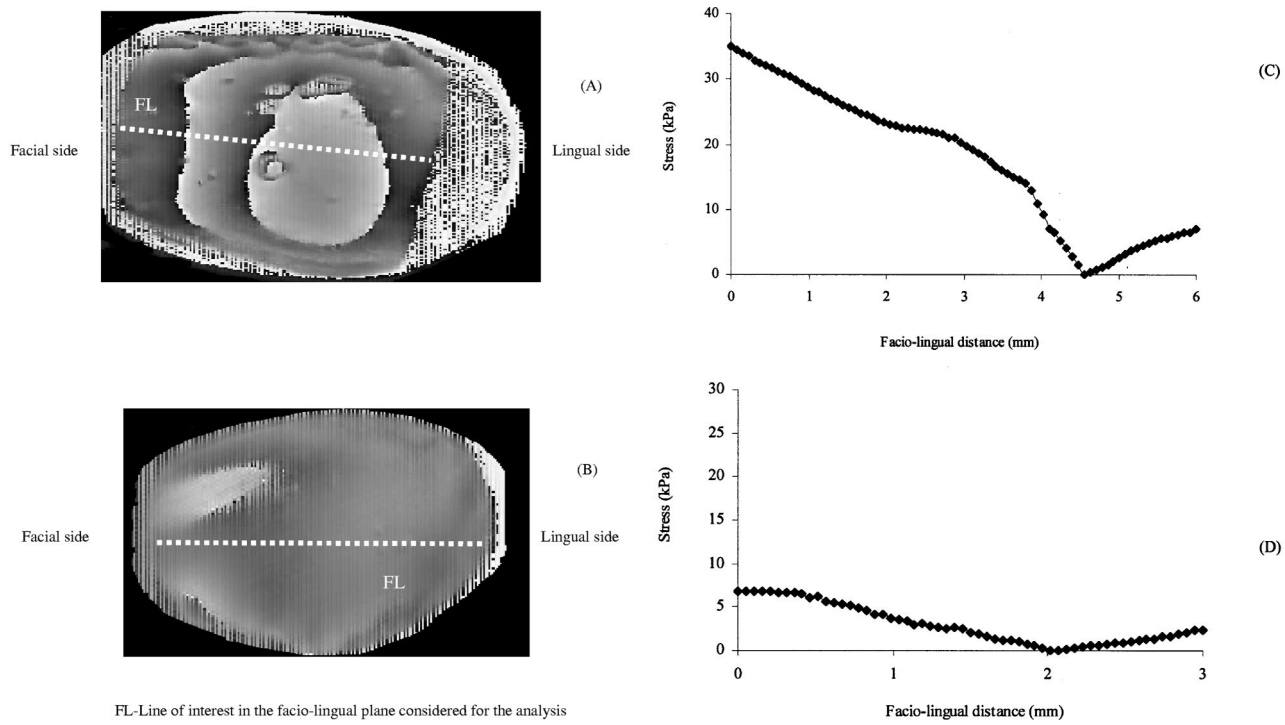

Fig. 7 Shows (a) the typical phase wrapped map at the cervical region (cross section) of the tooth model and (b) the typical phase wrapped map at the apical region (cross section) of the tooth model. (c) The typical graph showing the stress distribution pattern at the cervical region (cross section) of the tooth model and (d) the typical graph showing the stress distribution pattern at the apical region (cross section) of the tooth model.

4 Discussion

Tooth is a vital biological structure, which has important mechanical requirements, particularly during mastication. Dentine forms the main bulk of the tooth structure, and the erupted portion of a tooth consists of mainly dentine (crown dentine) which is covered by enamel, while, the portion of the tooth that rest within the socket of the jaw bone, also consists of mainly dentine (root dentine), and is covered by cementum. The root dentine serves as an interface between the supporting bone and crown dentine, and is primarily responsible for the distribution of functional stresses from the tooth to the supporting alveolar bone.[17] The crown dentine forms the interface between root dentine and enamel. From a materials science perspective, dentine can be cited as a biologically graded material that facilitates efficient transfer of mechanical stresses and strains to the supporting bone. The stress and strain analyses conducted in this study was meant to rationalize the role of material property organization on the stress-strain distribution within dentine.

The purpose of this study was to investigate the patterns of strain in macrostructural dentine, and all the specimens showed the same nature of gradients in strains. Determining the absolute value of strain was not the focus of this study. The three-dimensional photoelasticity displayed distinct bending stresses in tooth structure at the coronal and cervical regions. Bending resulted in conspicuous stress distribution along the faciolingual plane in the dentine. These stresses were minimal in the inner region and increased towards the facial and lingual surfaces. There was no bending or similar stress distribution in the apical dentine. This distinct nature of stress distribution had close agreement with the two-dimensional stress distribution observed in tooth model (sagittal section), and the spatial gradients in elastic modulus and pattern of mineralization in dentine structure.[14] This finding formed the basis of the sectional tooth model used for the present moiré interferometric analysis. It should be noted that the elastic modulus within a biological structure such as dentine is not homogeneous. Yet in this study we used photoelastic models with isotropic properties to study the pattern of stress distribution. This approach aided in understanding the stress distribution pattern in a tooth structure with isotropic properties. Since the moiré interferometry displayed strain patterns in natural dentine structure, the results obtained from the stress analysis on isotropic photoelastic models were useful to comprehend the influence of natural material organization on stress-strain distribution.

The digital moiré analysis showed major strains at the cervical dentine during compression. The observed strains were normal and shear in nature. The cervical dentine on the facial side exhibited maximum shear components of the axial and lateral strains, and this might be a contributing factor for abfraction lesions.[19] In addition, there was a conspicuous reduction in strains towards the apical dentine, and this difference in strains between the cervical and apical dentine was prominent for initial loads. This finding corresponded with our previous finding from *in vivo* experiments, which demonstrated significant strain reduction towards the apical region.[20] The apical dentine in this study showed distribution of only normal axial and lateral strains. It is interesting to note that the root dentine is structurally and compositionally different from coronal dentine.[21] During testing, the tooth specimens were maintained hydrated only until grating replication, and this

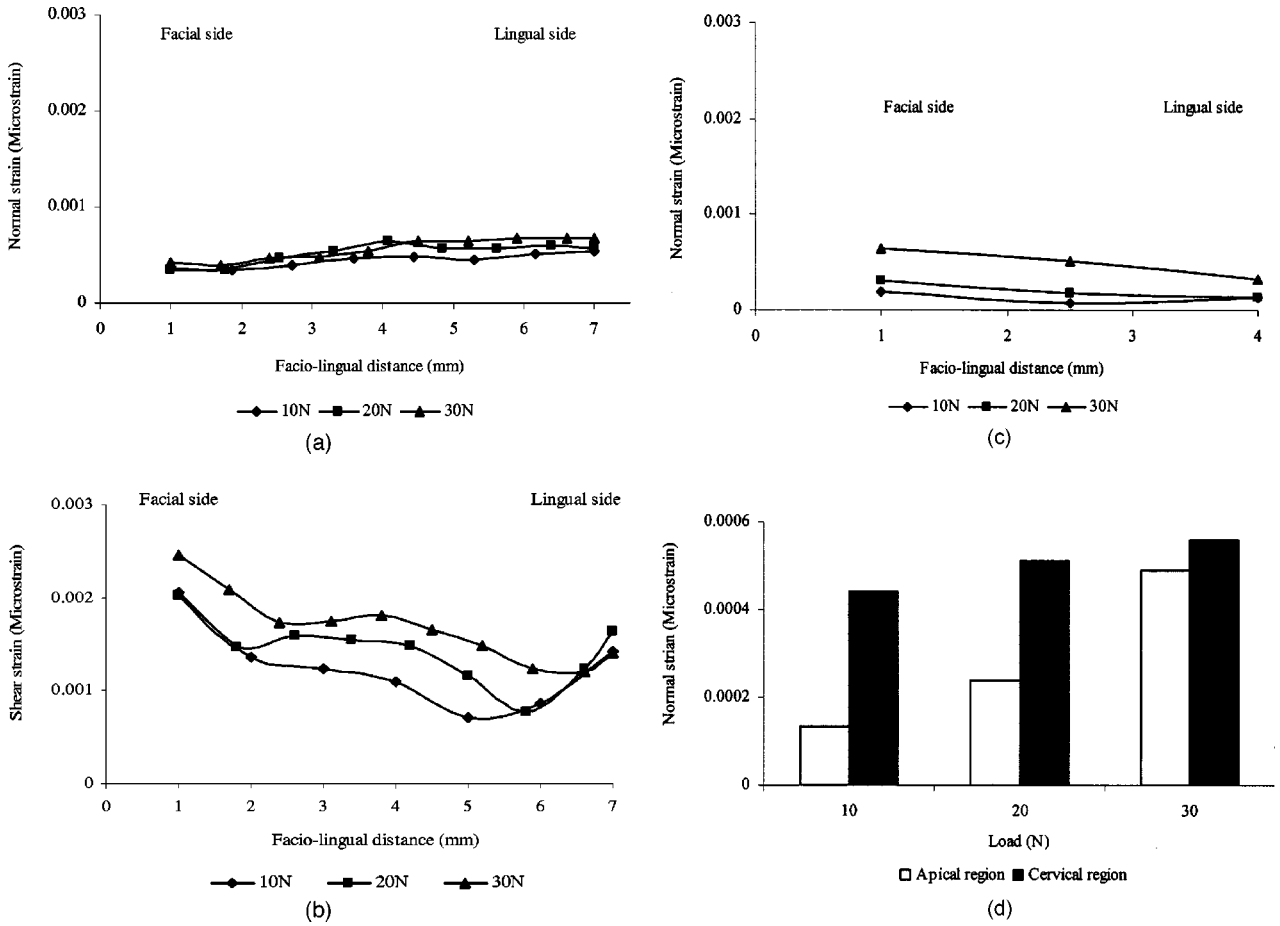

Fig. 8 Typical graphs obtained from the *U* field analysis showing (a) the normal strain and (b) the shear strain distribution in the axial direction at the cervical dentine, (c) the normal strain distribution in the axial direction at the apical region, and (d) the normal strains in the axial direction at the cervical and apical dentine.

will lead to the loss of certain amount of water from dentine. Our pilot experiments have shown that this process of dehydration would lead to the loss of less than 3% of water, while the remaining 10%–12% of water will remain in the dentine matrix. This finding corresponded with the values on ''water loss'' reported by Jameson et al.[12] Previous investigations using moiré interferometry have shown that extensive moisture loss produced fairly constant strains through out the bulk of the dentine.[22]

In this moiré interferometric analysis, grating was replicated on a sagittal surface of the tooth specimen. A technique recommended by Post et al.[18] was employed in this study. Similar approach of grating replication on dentine surface were reported in earlier studies also.[22,23] It is important to note that the major portion of the dentinal tubules in this section extends faciolingually and they will be parallel to the grating-replicated surface. This mode of specimen preparation would minimize epoxy adhesive from penetrating into the dentinal tubules. However, more research is warranted to understand the effect of this adhesive on dentine. Furthermore, biting loads between 10 and 30 N were applied in this study. These loads were selected due to the following reasons: (1) biting forces that occur during chewing are considerably lower than maximum bite forces. Although maximum axial loads up to 150 N have been recorded during chewing, in most cases the chewing force did not exceed 10 N.[24,25] (2) To avoid long experimentation time and to minimize subsequent load-induced time-dependent changes, and room-temperature dehydration-effect on dentine.[26,27]

Having observed a distinct pattern of stress distribution and strain gradients within structural dentine, an attempt is made in the following paragraph to rationalize why natural tooth adapts such a complex structure-to-material property relationship. The primary requirement of tooth is to function as a mechanical device during various masticatory activities. Consequently, it tries to enhance its performance within the anatomical confinement as any well-engineered structure. The process of enhancing the endurance limit of dentine is seemingly complicated because of the different oral habits and varying loads acting on the tooth. It is established in structural engineering that for a longer fatigue life span one would need to minimize stress concentrations and facilitate uniform distribution of strain. The ''performance enhancement'' in tooth structure is mainly achieved through material organization, which satisfies the functional requirements of the tooth and improves its compatibility with the supporting bone.

The present stress analysis showed higher stress distribution towards the outer aspects (facial and lingual sides) of the dentine structure. Our previous experiments have demonstrated higher elastic modulus in these regions.[14] Stiffening of

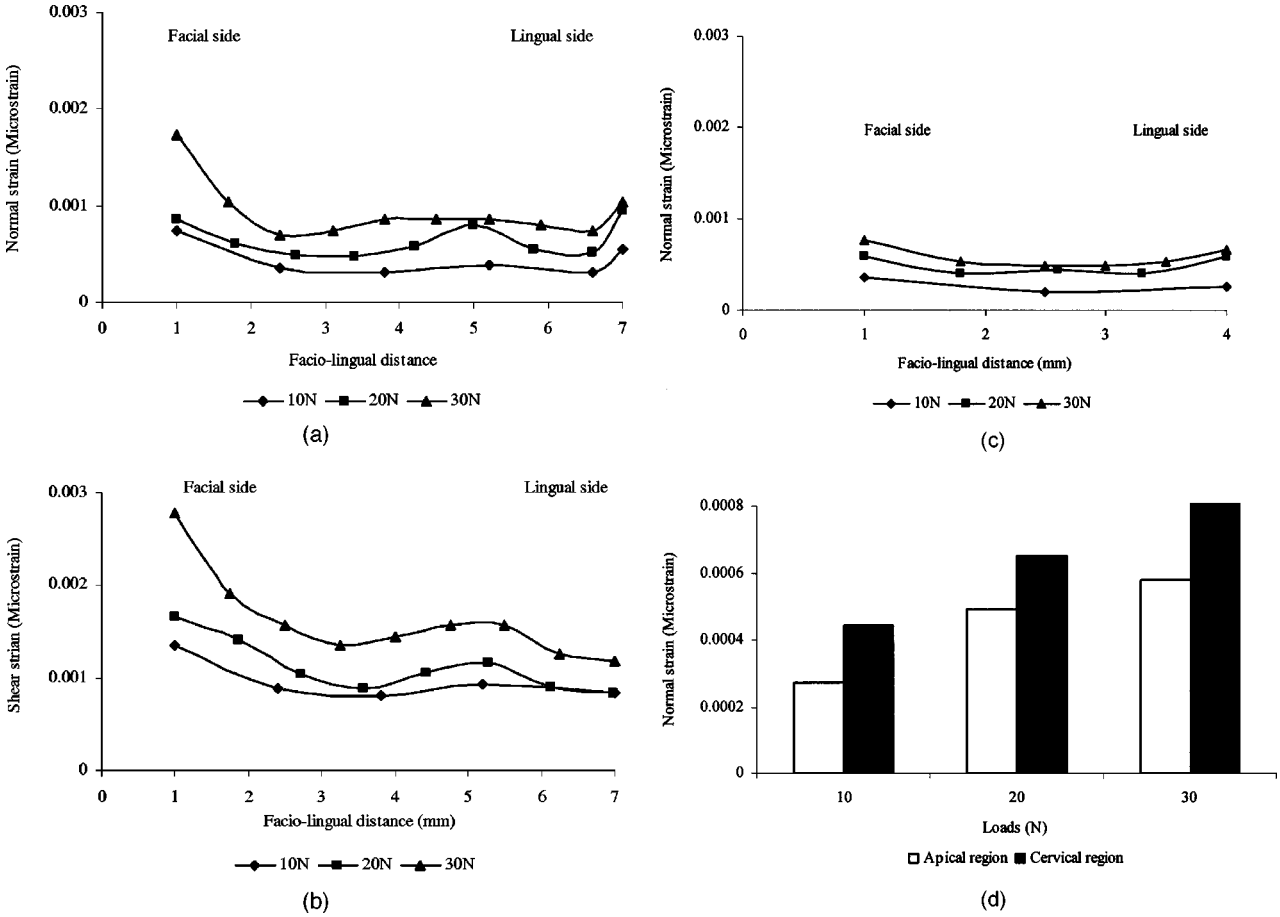

Fig. 9 Typical graphs obtained from the *V* field analysis showing (a) the normal strain and (b) the shear strain distribution in the lateral direction at the cervical dentine, (c) the normal strain distribution in the lateral direction at the apical region, and (d) the normal strain distribution in the lateral direction at the cervical and apical dentine.

the outer aspect of the dentine produced lesser strains in the graded material compared to the homogeneous material. This finding corresponded with our earlier studies and the strain-hardness relationship reported by Wang and Weiner.[14,28] If we assume that dentine is made up of homogeneous isotropic material, then this structure would display bending stress as demonstrated by the photoelastic experiment. This bending stress would result in steep gradients in stresses from low in the inner core dentine to high in the outer dentine. Since this is unfavorable for dento-osseous system, the dentine organizes by grading its material properties. The material property gradient in natural dentine contributed to the uniform distribution of strains in the root dentine. The gradients in elastic modulus may also enhance damage tolerance through strain distribution as shown by Suresh, based on their experiments on microscopically graded composite materials.[29] This process of mineralization and stiffening would not only improve the mechanical properties in appropriate locations but also makes the tooth lighter in weight. It is concluded from this experimental investigation that complex spatial gradation of material properties caused a distinct and homogenous strain gradients within dentine structure. This pattern of strain gradients will enhance the endurance of dentine structure and improves compatibility of the tooth-bone interface.

References

1. G. W. Marshall, Jr., S. J. Marshall, J. H. Kinney, and M. Balooch, ''The dentin substrate: structure and properties related to bonding,'' *J. Dent.* **25**, 441–458 (1997).
2. A. Kishen and A. Asundi, ''Photomechanical investigations on post-endodontically rehabilitated teeth,'' *J. Biomed. Opt.* **7**, 262–270 (2002).
3. L. E. Lanyon, A. E. Goodship, C. J. Pye, and J. H. MacFie, ''Mechanically adaptive bone remodeling,'' *J. Biomech.* **15**, 141–154 (1982).
4. H. M. Frost, ''Skeletal structural adaptations to mechanical usage (SATMU): 1. Redefining Wolff's law: the bone modeling problem,'' *Anat. Rec.* **226**, 403–413 (1990).
5. J. G. Skedros, M. W. Mason, M. C. Nelson, and R. D. Bloebaum, ''Evidence of structural and material adaptation to specific strain features in cortical bone,'' *Anat. Rec.* **246**, 47–63 (1996).
6. C. T. Rubin and L. E. Lanyon, ''Regulation of bone mass by mechanical strain magnitude,'' *Calcif. Tissue Int.* **37**, 411–417 (1985).
7. J. H. Kinney, M. Balooch, G. W. Marshall, and S. J. Marshall, ''A micromechanics model of the elastic properties of human dentine,'' *Arch. Oral Biol.* **44**, 813–822 (1999).
8. S. Weiner, A. Veis, E. Beniash, T. Arad, J. W. Dillon, B. Sabsay, and F. Siddiqui, ''Peritubular dentin formation: crystal organization and the macromolecular constituents in human teeth,'' *J. Struct. Biol.* **126**, 27–41 (1999).
9. W. Tesch, N. Eidelman, P. Roschger, F. Goldenberg, K. Klaushofer, and P. Fratzl, ''Graded microstructure and mechanical properties of human crown dentin,'' *Calcif. Tissue Int.* **69**, 147–157 (2001).
10. J. H. Kinney, S. Habelitz, S. J. Marshall, and G. W. Marshall, ''The

importance of intrafibrillar mineralization of collagen on the mechanical properties of dentin,'' *J. Dent. Res.* **82**, 957–961 (2003).
11. J. H. Kinney, S. J. Marshall, and G. W. Marshall, ''The mechanical properties of human dentin: a critical review and re-evaluation of the dental literature,'' *Crit. Rev. Oral Biol. Med.* **14**, 13–29 (2003).
12. M. W. Jameson, B. G. Tidmarsh, and J. A. Hood, ''Effect of storage media on subsequent water loss and regain by human and bovine dentine and on mechanical properties of human dentine *in vitro*,'' *Arch. Oral Biol.* **39**, 759–767 (1994).
13. E. Beniash, W. Traub, A. Veis, and S. Weiner, ''A transmission electron microscope study using vitrified ice sections of predentin: structural changes in the dentin collagenous matrix prior to mineralization,'' *J. Struct. Biol.* **132**, 212–225 (2000).
14. A. Kishen, U. Ramamurty, and A. Asundi, ''Experimental studies on the nature of property gradients in human dentine,'' *J. Biomed. Mater. Res.* **51**, 650–659 (2000).
15. J. W. Dally and W. F. Riley, *Experimental Stress Analysis*, 3rd ed., McGraw-Hill, New York (1991).
16. ''Measurements Group,'' in *Instruction for using photoelastic liquid plastic type PLM-1. Instruction bulletin IB-204-A*, Photoelastic division, Measurements Group, Inc., Raleigh, NC 27611.
17. A. Asundi and A. Kishen, ''Digital photoelastic investigations on the tooth-bone interface,'' *J. Biomed. Opt.* **6**, 224–230 (2001).
18. D. Post, B. Han, and P. Ifju, *High Sensitivity Moiré: Experimental Analysis for Mechanics & Materials*, Springer, New York (1994).
19. J. S. Rees, ''The role of cuspal flexure in the development of abfraction lesions: a finite element study,'' *Eur. J. Oral Sci.* **106**, 1028–1032 (1998).
20. A. Asundi and A. Kishen, ''A strain gauge and photoelastic analysis of *in vivo* strain and *in vitro* stress distribution in human dental supporting structures,'' *Arch. Oral Biol.* **45**, 543–550 (2000).
21. A. R. Ten Cate, *Oral Histology: Development, Structure and Function*, 5th Ed., Mosby, Inc. St. Louis (1998).
22. J. D. Wood, R. Wang, S. Weiner, and D. H. Pashley, ''Mapping of tooth deformation caused by moisture change using moiré interferometry,'' *Dent. Mater.* **19**, 159–166 (2003).
23. A. Kishen and A. Asundi, ''Investigations of thermal property gradients in the human dentine,'' *J. Biomed. Mater. Res.* **55**, 121–130 (2001).
24. D. J. Anderson, ''Measurement of stress in mastication I,'' *J. Dent. Res.* **35**, 664–670 (1956).
25. D. J. Anderson, ''Measurement of stress in mastication II,'' *J. Dent. Res.* **35**, 671–673 (1956).
26. J. Jantarat, J. E. Palamara, C. Lindner, and H. H. Messer, ''Time-dependent properties of human root dentin,'' *Dent. Mater.* **18**, 486–493 (2002).
27. J. F. Bates, G. D. Stafford, and A. Harrison, ''Masticatory function—a review of the literature. 1. The form of the masticatory cycle,'' *J. Oral Rehabil.* **2**, 281–301 (1975).
28. R. Z. Wang and S. Weiner, ''Strain-structure relations in human teeth using moiré fringes,'' *J. Biomech.* **31**, 135–141 (1998).
29. S. Suresh, ''Graded materials for resistance to contact deformation and damage,'' *Science* **29**, 2447–2451 (2001).